

Recycling diverse models for out-of-distribution generalization

Alexandre Ramé^{1,2}, Kartik Ahuja¹, Jianyu Zhang^{1,3},
Matthieu Cord^{2,4}, Léon Bottou^{1,3}, David Lopez-Paz¹

¹Meta AI, Paris, France ²Sorbonne Université, CNRS, ISIR, Paris, France

³NYU, New-York, USA ⁴Valeo.ai, Paris, France

Abstract

Foundation models are redefining how AI systems are built. Practitioners now follow a standard procedure to build their machine learning solutions: download a copy of a foundation model, and fine-tune it using some in-house data about the target task of interest. Consequently, the Internet is swarmed by a handful of foundation models fine-tuned on many diverse tasks. Yet, these individual fine-tunings often lack strong generalization and exist in isolation without benefiting from each other. In our opinion, this is a missed opportunity, as these specialized models contain *diverse* features. Based on this insight, we propose *model recycling*, a simple strategy that leverages multiple fine-tunings of the same foundation model on diverse auxiliary tasks, and repurposes them as rich and diverse initializations for the target task. Specifically, model recycling fine-tunes in parallel each specialized model on the target task, and then averages the weights of all target fine-tunings into a final model. Empirically, we show that model recycling maximizes model diversity by benefiting from diverse auxiliary tasks, and achieves a new state of the art on the reference DomainBed benchmark for out-of-distribution generalization. Looking forward, model recycling is a contribution to the emerging paradigm of *updatable machine learning* where, akin to open-source software development, the community collaborates to incrementally and reliably update machine learning models.

1 Introduction

The framework of *foundation models* [1] is fueling a spectacular adoption of machine learning for real-world applications. Foundation models (also known as pre-trained models) are machine learning systems trained on large-and-diverse data [2, 3, 4], which are easy to adapt to downstream tasks. Having ditched the “training from scratch” mentality, practitioners now follow a standardized two-step transfer learning strategy [5, 6, 7]. First, the practitioner downloads a copy of some foundation model, often provided by authorities such as `torchvision` [8] or `huggingface` [9]. Second, the practitioner fine-tunes the weights on their target task, by leveraging a limited amount of in-house data. Unfortunately, each of these fine-tunings risks latching onto specific patterns from the practitioner’s training data [10, 11, 12, 13]. Therefore, these shortsighted models fail to generalize when presented with out-of-distribution (OOD) test examples [14, 15, 16, 17], which can result in negative impact on human lives [18, 19].

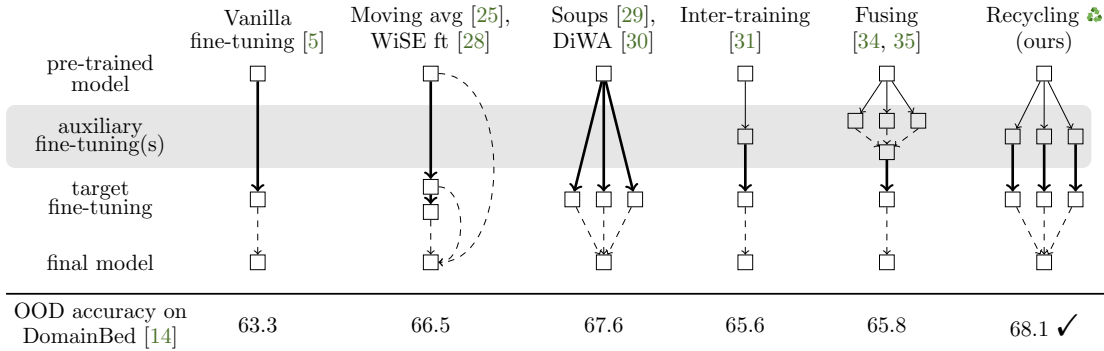


Figure 1: The different training strategies discussed in this paper. They all start with a pre-trained foundation model, often provided by some authority such as `torchvision` [8] or `huggingface` [9]. Some of the training strategies fine-tune the pre-trained model on auxiliary tasks (thin solid arrows \longrightarrow): these auxiliary fine-tunings can be performed by different contributors of the community on their own data. Then, all strategies perform fine-tuning on the target task of interest (thick solid arrows \rightarrow). Finally, the weights fine-tuned on the target task are used as is, or are weight-averaged into a final model (dashed arrows $- \rightarrow$). Our proposed *model recycling* is attractive because it (i) enables compute parallelism throughout auxiliary and target fine-tunings, (ii) maximizes the amount of diversity in the predictions of the fine-tuned models, (iii) achieves state-of-the-art performance in DomainBed [14], the standard benchmark for OOD generalization and (iv) is without any inference or training overhead compared to a traditional hyperparameter search.

Increased OOD generalization would enable the responsible use of machine learning in applications where robustness and safety are critical, such as medical imaging [20, 21] and autonomous driving [22, 23]. Thus how to best fine-tune foundation models for OOD generalization is becoming a central topic of research [24]. In particular, the recently discovered ability to average neural networks’ weights [25, 26] has inspired a plethora of modern fine-tuning approaches. We illustrate some of them in Figure 1, such as moving averages [25, 27], WiSE fine-tuning [28], Model Soups [29] and DiWA [30]. However, these strategies ignore the swarms of “specialized fine-tunings” of the same foundation model increasingly available in the Internet. In contrast, the inter-training [31, 32, 33, 34] and fusing [34, 35] strategies include intermediate fine-tunings on auxiliary tasks to enrich the features and the initialization for the target downstream task; yet, they heavily depend on the similarity between the auxiliary and target tasks, and fail to best leverage the diversity in the auxiliary weights (as argued in Section 2).

Motivated by the empirical and theoretical evidence showing that diversity improves generalization [36, 37, 38, 39, 40, 30], we ask:

How can we best reuse the diverse fine-tunings of the same foundation model to train a model with strong out-of-distribution performance on our target task?

Our answer to this question is a simple fine-tuning strategy we call *model recycling* (Section 3), illustrated in Figure 1. In a similar fashion to converting waste into reusable material for new uses, we take fine-tunings of the same foundation model on diverse auxiliary tasks and repurpose them into initializations to start multiple fine-tunings on the target task. In a nutshell, model recycling is a three-step process, namely (i) fine-tune a copy of the foundation model on each auxiliary task, (ii) fine-tune each auxiliary model on the target task, and (iii) return as the final model the average of all target fine-tunings. Recycling enables compute parallelism throughout training. It is efficient because it leverages the auxiliary tasks to increase predictive diversity, and constructs a final model with decreased over-fitting to task-specific patterns.

We show the efficacy of model recycling in Section 4, where we set a new state of the art on DomainBed [14], the reference benchmark evaluating OOD generalization. As we discuss in our closing Section 5, this work contributes to the emerging paradigm of *updatable machine learning* [41], where practitioners work in collaboration towards incrementally and reliably updating the capabilities of a machine learning model. As also highlighted in recent works [33, 34], we envision a future where deep neural networks are trained by following similar pipelines to the ones in open-source development with version control systems.

2 Fine-tuning for out-of-distribution generalization

We start by describing our learning setup. We are concerned with learning a deep learning model $f_\theta = f_w \circ f_\phi$, where the featurizer f_ϕ is parametrized by the weights ϕ , the classifier f_w is parametrized by the weights w , and the joint model f_θ is parametrized by the concatenation weights $\theta = (w, \phi)$. While both train and test data correspond to the same target task—for instance, classifying images into a fixed set of categories—we allow a distribution shift between the two. Formally, we are dealing with the problem of out-of-distribution (OOD) generalization, and our aim is to find a θ maximizing the test accuracy $\text{acc}_{\text{te}}(\theta)$.

2.1 Vanilla fine-tuning

Turns out, the vanilla *fine-tuning* [5] baseline is frustratingly difficult to beat in this task [14]. Fine-tuning is a simple recipe, namely (i) download a pre-trained featurizer with parameters ϕ^{pt} , (ii) plug a classifier w^{lp} compatible with the target task, and (iii) fine-tune the model using empirical risk minimization (ERM) [42] on the target task. While the classifier w^{lp} could be initialized at random, first learn only the classifier with frozen featurizer (i.e., linear probing) on the target task improves results by preventing feature distortion [24]. This fine-tuning strategy is the standard practice to transfer the knowledge from models pre-trained on ImageNet [43] towards various datasets—notably those with the presence of distribution shift, for example PACS [44], VLCS [45], OfficeHome [46], TerraIncognita [47] and DomainNet [48]. Since successful fine-tuning critically depends on the scale and diversity of the pre-training corpus [2, 3, 49], authorities such as `torchvision` [8] or `huggingface` [9] started maintaining public repositories of high-quality pre-trained models [1]. Most users, particularly those with modest computation resources, now simply download these pre-trained models, and adapt them swiftly to their interests.

2.2 Weight averaging over epochs

For years, vanilla fine-tuning remained the reigning strategy to train robust models. This was until the very first techniques on *weight averaging* came to the foreground [25, 50]. While fine-tuning a pre-trained model, they saved checkpoints every few epochs and built a final model whose weights were the average of those multiple checkpoints. Due to the nonlinear nature of deep neural networks, this was a surprising observation that [51] called the linear mode connectivity:

Observation 1 (LMC with different epochs [25]) *Two weights θ_a and θ_b , obtained at two different epochs of the same fine-tuning, satisfy the linear mode connectivity (LMC):*

$$\text{acc}_{\text{te}}((1 - \lambda) \cdot \theta_a + \lambda \cdot \theta_b) \gtrsim (1 - \lambda) \cdot \text{acc}_{\text{te}}(\theta_a) + \lambda \cdot \text{acc}_{\text{te}}(\theta_b) \text{ for all } \lambda \in [0, 1].$$

The LMC holds if the accuracy of the interpolated weights is above the interpolated accuracy. This definition is more restrictive than in the literature; for example, [51] only requires less than 2% in error increase with regard to the worst endpoints. Consistently with this Observation 1, weight averaging strategies [27, 28, 52] improved performance in OOD classification.

2.3 Weight averaging over runs

Perhaps motivated by these results, Neyshabur, Sedghi, and Zhang [26] pushed the envelope of weight averaging techniques, and obtained the following insight:

there is no performance barrier between two instances of models trained from pre-trained weights, which suggests that the pre-trained weights guide the optimization to a flat basin of the loss landscape [...] Moreover, interpolating two random solutions from the same basin could generally produce solutions closer to the center of the basin, which potentially have better generalization performance than the endpoints.

Two *independent* fine-tunings—differing in hyperparameter choices, data access order, and other stochastic factors—starting from the same pre-trained model also satisfy the LMC! Formally,

Observation 2 (LMC with different runs [26, 51]) *The LMC holds between θ_a and θ_b fine-tuned on the target task initialized from a shared pre-trained model.*

See Figure 2a for an illustration of Observations 1 and 2. Observation 2 inspired Model Soups [29] and DiWA [30]—the current state-of-the-art approaches for OOD generalization—to average the weights obtained from an hyperparameter search. However, the shared initialization constraint limits models diversity [53, 54], especially when compared to methods that can combine arbitrary networks, for example via prediction averaging in deep ensembles [55].

2.4 Weight averaging over tasks

All the methods described so far directly fine-tune some pre-trained model on the training task. Could external datasets, increasingly available online, be incorporated into the learning process to learn richer features? Such *auxiliary* tasks could be an opportunity to recruit specialized features that match our target task, ease optimization [39, 40], or “offer some high-level guidance to bridge the gaps between the pre-training and fine-tuning phases” [56]. Following these ideas, inter-training [31, 32, 33] performs an *intermediate fine-tuning* of the pre-trained model on some auxiliary task, before tackling the target task. However, the sequential nature of inter-training leads to the catastrophic forgetting [57] of some useful knowledge contained in the original pre-trained model; moreover, the choice of the auxiliary task plays a determinant role, since “when the wrong task is chosen, inter-training hurts results” [35].

To address the shortcomings of inter-training, recent works [34, 35] have introduced *fusing* strategies able to accommodate multiple auxiliary tasks. The recipe for fusing is to (i) fine-tune one copy of the pre-trained model on each auxiliary task, (ii) average the auxiliary fine-tuning weights, and (iii) use such averaged model as the initialization for the target fine-tuning. See Figure 1 for an illustration comparing all these fine-tuning strategies. Fusing held great promise to extract rich features from diverse auxiliary tasks, yet it only provides marginal gains in standard OOD generalization benchmarks such as DomainBed (see Section 4.1). We posit that model fusing is performing weight averaging prematurely, destroying most diversity from auxiliary tasks even before the target task can benefit from it. To address these issues, next we propose *model recycling*, a new fine-tuning strategy that performs one target fine-tuning per auxiliary weights, and averages weights only as the very last step.

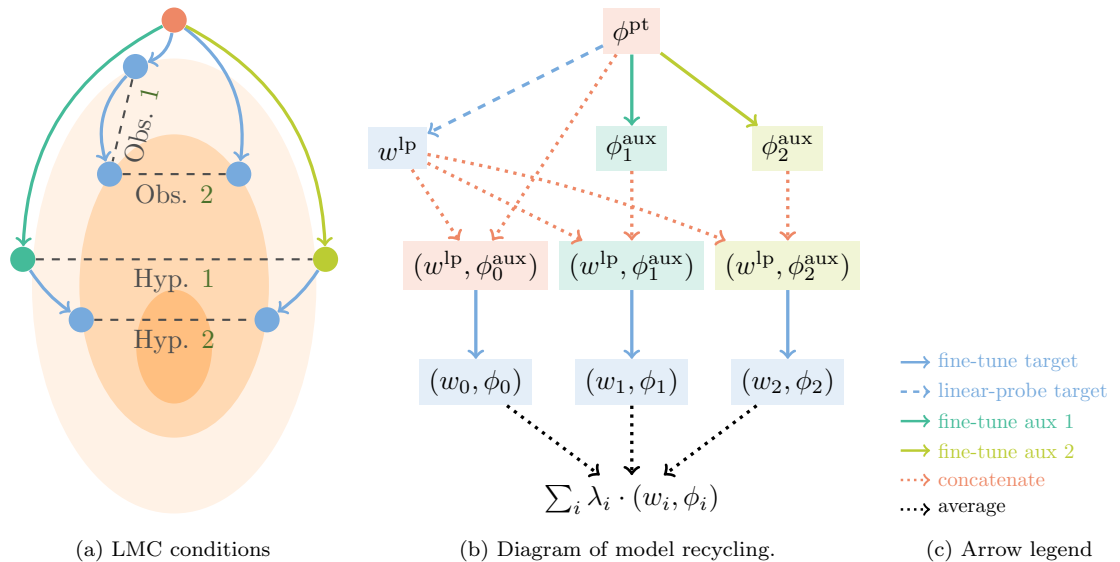


Figure 2: Illustrations of (a) different linear mode connectivity (LMC) conditions, and (b) model recycling. In subplot (a), we illustrate Observation 1, about LMC between two checkpoints along the same target fine-tuning; Observation 2, about LMC between two target fine-tunings; Hypothesis 1, about LMC between two auxiliary fine-tunings; and Hypothesis 2, about LMC between two target fine-tunings initialized from auxiliary weights satisfying Hypothesis 1. In subplot (b), we offer a diagram of our proposed model recycling, where we (i) fine-tune a pre-trained model on auxiliary tasks, (ii) plug a linear probe on the pre-trained model and the auxiliary fine-tunings, (iii) fine-tune on the target task from each auxiliary weights, and (iv) return their weight average as the final model.

3 Model recycling

Model recycling is a proposal to leverage diverse auxiliary fine-tunings of the same pre-trained model; it is compared against other fine-tuning strategies in Figure 1 and outlined in detail in Figure 2b. We can describe model recycling by the following 5-steps and parallelizable procedure.

1. Download an appropriate featurizer ϕ^{pt} , pre-trained on task T_0 .
2. Fine-tune ϕ^{pt} on each auxiliary task T_i , obtaining $(w_i^{\text{aux}}, \phi_i^{\text{aux}})$ for $i = 0, \dots, k$.
3. Replace each w_i^{aux} by w^{lp} , obtained by linear probing the original pre-trained model ϕ^{pt} on the target task T . This shared linear probe classifier facilitates LMC by preventing feature distortions [24].
4. Fine-tune each $(w^{\text{lp}}, \phi_i^{\text{aux}})$ on the target task T , obtaining $\theta_i = (w_i, \phi_i)$ for $i = 0, \dots, k$.
5. Return as final model the linear combination $\sum_{i=0}^k \lambda_i \cdot \theta_i$. Following [29, 30], we compare two approaches to select the interpolating coefficients. The first “uniform” averages $\lambda_i = \frac{1}{k}$. The second “greedy selection” sorts the θ_i by descending accuracy on the in-distribution (ID) validation dataset; then, it greedily iterates to construct a uniform average containing θ_i if and only if its addition lowers the ID validation accuracy.

We included the first two steps for completeness, but they are not needed when auxiliary fine-tunings are available online. Our strategy *recycles* auxiliary fine-tunings (that would otherwise ignore each other or be discarded) as diverse initializations to parallel fine-tunings on the

target task. We do not rely on intrinsically good auxiliary tasks [58, 59], but rather on diverse initializations with complementary knowledge. Note that we consider the pre-training task as the auxiliary task “number zero”. This resembles WiSE fine-tuning [28] and aims at preserving the general-purpose information contained in the original pre-trained model. More generally, recycling connects some of the fine-tuning strategies from Section 2 while overcoming their limitations. When compared to Model Soups [29] and DiWA [30], recycling removes the shared initialization constraint and thus benefits from the additional diversity brought by the different initializations specialized on various auxiliary tasks. When compared to inter-training [31] and fusing [34, 35], recycling avoids the difficult choice of choosing one single initialization. Moreover, when compared to fusing, recycling is an attractive strategy to combine knowledge from multiple tasks because it delays the weight averaging—and in turn, destruction of diversity.

New linear mode connectivity conditions. If model recycling is to work, it requires a relaxation of the conditions under which the LMC holds. To begin with, we introduce Hypothesis 1 to posit LMC between two models whose featurizers were fine-tuned on different auxiliary tasks.

Hypothesis 1 (LMC with different tasks) *The LMC holds between (w, ϕ_a^{aux}) and (w, ϕ_b^{aux}) if ϕ_a^{aux} and ϕ_b^{aux} are fine-tuned on two auxiliary tasks initialized from the same pre-trained featurizer ϕ^{pt} . Here, w is the linear probe of ϕ^{pt} on the target task.*

Though this Hypothesis 1 was never formulated explicitly, it is underlying in fusing approaches [34, 35, 60]. Model recycling requires the following additional Hypothesis 2.

Hypothesis 2 (LMC with different initializations) *The LMC holds between θ_a and θ_b fine-tuned on the target task initialized from (w, ϕ_a^{aux}) and (w, ϕ_b^{aux}) satisfying Hypothesis 1.*

This novel Hypothesis 2 is the first to state the LMC between weights fine-tuned from different initializations. It hints towards a more general inheritance property of LMC: if two initializations satisfy LMC, then the two final weights would too. We expect Hypotheses 1 and 2 to hold as long as the pre-training, auxiliary and target tasks are sufficiently similar.

To reiterate, diversity was shown to be positively correlated with strong generalization [36, 37, 38, 39, 40, 30]. Therefore, if Hypotheses 1 and 2 are true, we expect model recycling to be a high performer in out-of-distribution generalization benchmarks. But these questions, we can only answer empirically through proper experimentation.

4 Experiments

We implement numerical experiments to support three main claims, sorted in decreased granularity. First, Section 4.1 showcases the state-of-the-art (SoTA) performance of model recycling in DomainBed [14], the standard to benchmark OOD generalization. Second, Section 4.2 illustrates how such performance gains arise from increased diversity across averaged models. Third, Section 4.3 provides empirical support for Hypotheses 1 and 2, the technical conditions enabling these results. In Appendix A, we discuss the application of recycling for ID tasks. Our code will be released at <https://github.com/facebookresearch/ModelRecycling>.

4.1 Recycling achieves state-of-the-art OOD performance

Setup. Our first array of experiments shows the SoTA performance of model recycling on DomainBed [14]. The benchmark contains five computer vision datasets for OOD generalization: PACS [44], VLCS [45], OfficeHome [46], TerraIncognita [47] and DomainNet [48]. Each of

Table 1: Accuracies (\%, \uparrow) on the DomainBed [14] benchmark evaluating OOD generalization. Model recycling sets a new SoTA by leveraging auxiliary tasks’ diversity. The selection column indicates the weight selection strategy. The symbol “*” indicates inference computational overhead in functional ensembling approaches. The symbol “ \dagger ” indicates the averaging of all weights across 3 data splits.

Algorithm	Selection	PACS	VLCS	OfficeHome	TerraInc	DomainNet	Avg	
ERM	ID val	85.5 ± 0.2	77.5 ± 0.4	66.5 ± 0.3	46.1 ± 1.8	40.9 ± 0.1	63.3	
CORAL [61]	ID val	86.2 ± 0.3	78.8 ± 0.6	68.7 ± 0.3	47.6 ± 1.0	41.5 ± 0.1	64.6	
SWAD [52]	Loss-aware trajectory	88.1 ± 0.1	79.1 ± 0.1	70.6 ± 0.2	50.0 ± 0.3	46.5 ± 0.1	66.9	
MA [27]	Uniform trajectory	87.5 ± 0.2	78.2 ± 0.2	70.6 ± 0.1	50.3 ± 0.5	46.0 ± 0.1	66.5	
Deep ensembles* [27]	Uniform	87.6	78.5	70.8	49.2	47.7	66.8	
DiWA [30] runs	ERM	85.9 ± 0.6	78.1 ± 0.5	69.4 ± 0.2	50.4 ± 1.8	44.3 ± 0.2	65.6	
	Ensemble*	Uniform	88.1 ± 0.3	78.5 ± 0.1	71.7 ± 0.1	50.8 ± 0.5	47.0 ± 0.2	67.2
	Model Soups/DiWA	Uniform	88.7 ± 0.2	78.4 ± 0.2	72.1 ± 0.2	51.4 ± 0.6	47.4 ± 0.2	67.6
	Model Soups/DiWA	Greedy	88.0 ± 0.3	78.5 ± 0.1	71.5 ± 0.2	51.6 ± 0.9	47.7 ± 0.1	67.5
	Model Soups/DiWA \dagger	Uniform \dagger	89.0	78.6	72.8	51.9	47.7	68.0
Our runs	Inter-training [31]	ID val	89.0 ± 0.0	77.7 ± 0.0	69.9 ± 0.6	46.7 ± 0.1	44.5 ± 0.1	65.6
	Ensemble* of inter-training	Uniform	89.2 ± 0.1	79.0 ± 0.2	72.7 ± 0.1	51.1 ± 0.3	47.2 ± 0.1	67.8
	Fusing [35]	ID val	88.0 ± 1.0	78.5 ± 0.8	71.5 ± 0.5	46.7 ± 1.8	44.4 ± 0.2	65.8
	Recycling	Uniform	89.5 ± 0.1	78.5 ± 0.1	73.1 ± 0.1	51.8 ± 0.4	47.5 ± 0.1	68.1
	Recycling	Greedy	90.5 ± 0.2	78.7 ± 0.2	73.4 ± 0.3	49.2 ± 0.9	47.7 ± 0.0	67.9
Our runs	Recycling \dagger	Uniform \dagger	89.8	78.3	73.5	52.0	47.7	68.3

these datasets contains multiple domains about the same classification task. For example, the domains in PACS are “Photos”, “Art”, “Cartoons”, and “Sketches”. Each domain is successively considered as the test while others are for training; we report the test accuracy averaged over all test domains. Following standard practice in DomainBed, we launch 20 runs for each domain for each dataset, with a ResNet-50 [62] pre-trained on ImageNet [43], hyperparameters sampled from Table 2 and linear probing [24]. This entire process is repeated for 3 random data splits. This experimental setup is further described in Appendix E.

Approaches. Model Soups/DiWA [29, 30] share the same “direct transfer learning” protocol as ERM (Empirical Risk Minimization), yet differ by the selection strategy. While ERM selects the model with highest ID validation accuracy out of the 20 runs, Model Soups/DiWA either uniformly weight average all models or greedily select some—as described in Section 3. Our new approaches leverage auxiliary tasks, here for simplicity the other datasets (with all their domains) from DomainBed. Specifically, for PACS, each run is inter-trained on one of the following auxiliary task: VLCS, OfficeHome, TerraIncognita, DomainNet, or ImageNet (which we consider as the auxiliary task “number zero”). Then, rather than selecting one single model, recycling applies the uniform or the greedy selection, without any training overhead; in brief, model recycling is to inter-training as Model Soups/DiWA is to ERM. The symbol \dagger indicates the averaging of all $60 = 20 \times 3$ weights from the 3 data splits—at the expense of losing error bars. Fusing averages multiple auxiliary weights but at initialization. Ensembling strategies perform functional averaging [55], with high inference overhead (indicated by the symbol *); in particular, we report the scores from [27] for the deep ensembles* [55] baseline of $M = 6$ models with different random classifier initializations. Finally, CORAL [61] is the best invariant approach; SWAD [52] and MA [27] average weights along one training trajectory but differ in their selection strategy.

Results. Table 1 summarizes our results on DomainBed, where model recycling achieves a new SoTA: recycling with uniform selection improves its DiWA equivalent by 0.5 points after averaging over all datasets. More precisely, recycling-uniform beats DiWA-uniform by 0.8 and 1.0 points on PACS and OfficeHome, while recycling-greedy outperforms DiWA-greedy by 2.5 and 1.9 points on these two datasets. While inter-training and fusing also succeed on PACS and OfficeHome, they fail on TerraIncognita, because all auxiliary tasks are distant from photos of

animals in the wild; in contrast, recycling-uniform improves DiWA-uniform from 51.4 to 51.8 on TerraIncognita despite this lack of similar auxiliary tasks. This highlights a critical strength of recycling: its robustness to the choice of auxiliary tasks (though selecting more adequate auxiliary tasks would improve results). On VLCS, recycling is also generally beneficial (as visible in the per-domain results from Appendix E.2), except on one domain where the LMC breaks (as shown in Figure 9b from Appendix D). For DomainNet, recycling is SoTA though the gains are small w.r.t. DiWA: we suspect this is because the initialization strategy becomes less critical for larger datasets [56] with more training epochs (see Figure 3b).

4.2 Recycling increases model diversity

In Figure 3, we now investigate how the diversity across models fine-tuned on the target task influences the OOD performance of their weight average. Here, we measure diversity with the prediction q-diversity [53], which increases when models predict differently and fail on different examples; this diversity measure is precisely defined in Appendix C, where we also arrive at similar conclusions using another diversity measure [54]. Following [30], let the target task be OfficeHome, with ‘‘Art’’ as the test OOD domain; we train on the ‘‘ClipArt’’, ‘‘Product’’ and ‘‘Photo’’ domains. We consider different models, either only pre-trained on ImageNet (as in Model Soups/DiWA), or also inter-trained on DomainNet.

First, we verify that inter-training influences the final models. Specifically, Figure 3a confirms that networks with different initializations are more diverse than networks initialized similarly. Then, Figure 3b verifies that this diversity gain comes from their initialization and remains along fine-tuning on the target task. Moreover, Figure 3c shows that diversity is positively linearly correlated with OOD generalization: specifically, we observe that having different initializations improves diversity and thus the accuracy of their weight average. Finally, in Figure 3d, we consider averaging M weights: a proportion $(1 - \mu)$ start directly from ImageNet, the others μ were inter-trained on DomainNet. In the simplest case $M = 2$, using one model from each initialization leads to maximum accuracy; more generally, the best performances are usually obtained around $\mu \approx 0.5$, where the final weight average has maximal access to diverse initializations.

In conclusion, each auxiliary task fosters the learning of diverse features [63]. Recycling increases diversity and improves performance [38, 39] by removing a key limitation of Model Soups [29] and DiWA [30]; the need for all fine-tunings to start from a shared initialization.

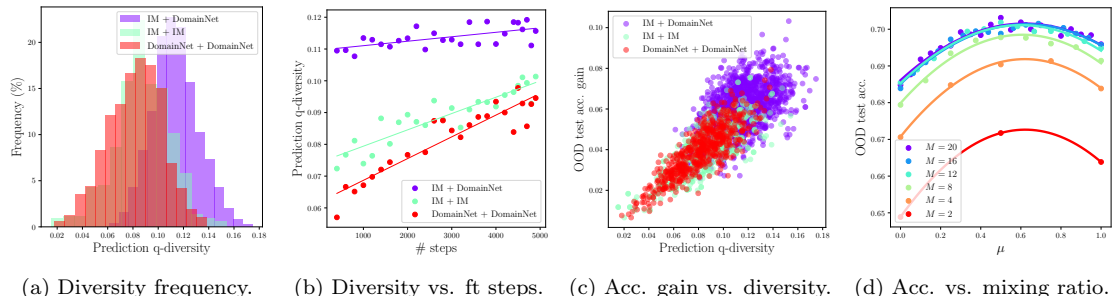


Figure 3: Explorations on q-diversity [53] and its positive impact on accuracy for the OOD test domain ‘‘Art’’ from OfficeHome. In (a), we compute the diversity between pairs of models either directly fine-tuned from ImageNet, either inter-trained on DomainNet: having one model from each initialization increases diversity. In (b), we plot this diversity along the 5k training steps. In (c), we observe that when two models are diverse, the accuracy of their weight average is higher than the average of their individual accuracies. In (d), we average M models: a proportion $(1 - \mu)$ start directly from ImageNet, the others μ are inter-trained on DomainNet. The accuracy of the weight average is maximized when $\mu \approx 0.5$.

4.3 Why recycling works? Analyzing Hypotheses 1 and 2

We conclude our experiments by providing empirical support for Hypotheses 1 and 2, and highlighting some failures in “extreme” conditions. In addition to the five datasets from DomainBed, for the sake of completeness, we thus also consider two very distant tasks; the medical RxRx [64] and Camelyon [65] from the WILDS [65] benchmark. For each target task, we consider the first domain as the test OOD; the other domains are used for training.

We validate Hypothesis 1 in Figures 4a to 4e. For each dataset, we plot the test OOD accuracy for the weights $(w^{\text{lp}}, (1 - \lambda) \cdot \phi_a^{\text{aux}} + \lambda \cdot \phi_b^{\text{aux}})$, where the classifier w^{lp} is a linear probe of the ImageNet pre-trained featurizer $\phi_{\text{IM}}^{\text{pt}}$, and $\lambda \in [0, 1]$ interpolates between ϕ_a^{aux} and ϕ_b^{aux} , obtained by fine-tuning on two auxiliary tasks initialized from $\phi_{\text{IM}}^{\text{pt}}$. First, we observe that task similarity influences OOD generalization since the test accuracies in Figure 4c agree with the fact that OfficeHome is most similar to DomainNet, not as similar to TerraIncognita, and most dissimilar to the medical dataset RxRx. Second, *the accuracy of the interpolated weights is above the interpolated accuracy*: this validates Hypothesis 1. The accuracy is even usually concave in λ .

Similarly, we analyze Hypothesis 2 on Figures 4f to 4j. For each dataset, we plot the test OOD accuracy for the model with weights $(1 - \lambda) \cdot \theta_a + \lambda \cdot \theta_b$, where the coefficient $\lambda \in [0, 1]$ interpolates between θ_a and θ_b , fine-tuned on the target task respectively starting from $(w^{\text{lp}}, \phi_a^{\text{aux}})$ and $(w^{\text{lp}}, \phi_b^{\text{aux}})$. We observe that Hypothesis 2 usually holds: for example, even recycling RxRx can help for OfficeHome on Figure 4h. Yet, Hypothesis 2 breaks on TerraIncognita and Camelyon in Figures 4i and 4j when RxRx is the auxiliary task. In light of these results, we argue that Hypothesis 2 holds as long as either the auxiliary or the target task is sufficiently similar to the pre-training task. We speculate this prevents feature distortion [24] and escaping a shared loss valley. In Appendix D, we further analyze Hypothesis 2, notably in a more complex setup where the intermediate tasks are successive fine-tunings on several auxiliary datasets. Better understanding when Hypothesis 2 breaks is a promising research direction; among other factors, we believe that larger pre-training corpus (as in [66]) or larger architectures (as in [34]) may help.

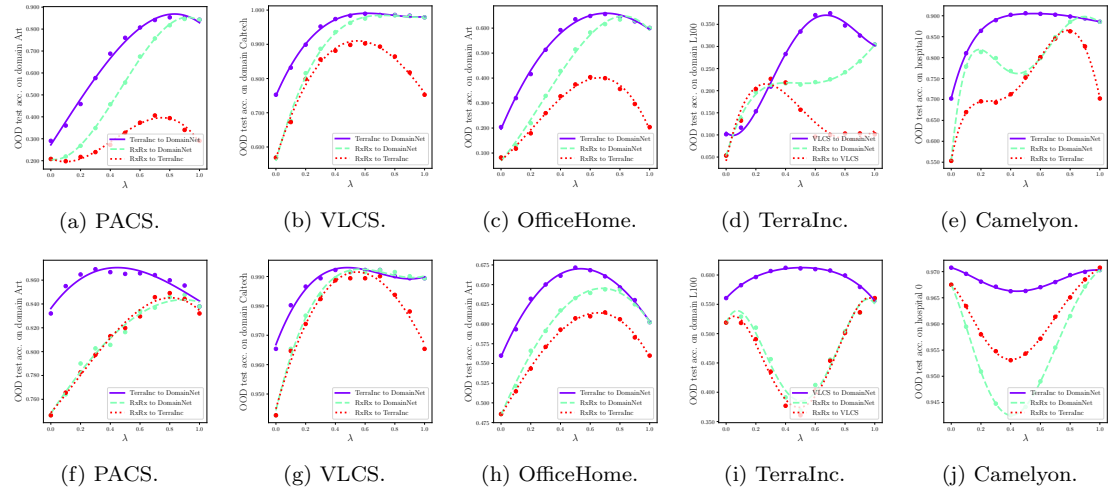


Figure 4: The first row validates Hypothesis 1 by plotting $\lambda \rightarrow \text{acc}_{\text{te}}((w^{\text{lp}}, (1 - \lambda) \cdot \phi_a^{\text{aux}} + \lambda \cdot \phi_b^{\text{aux}}))$, where w^{lp} is the linear probe of $\phi_{\text{IM}}^{\text{pt}}$, and ϕ_a^{aux} and ϕ_b^{aux} are fine-tuned on the two auxiliary datasets in the legend “Dataset_a to Dataset_b”. The second row supports Hypothesis 2 by plotting $\lambda \rightarrow \text{acc}_{\text{te}}((1 - \lambda) \cdot \theta_a + \lambda \cdot \theta_b)$ where θ_a and θ_b are fine-tuned on the target task starting respectively from $(w^{\text{lp}}, \phi_a^{\text{aux}})$ and $(w^{\text{lp}}, \phi_b^{\text{aux}})$. We encounter two exceptions to Hypothesis 2 (Figures 4i and 4j), due to the fact that *neither* the auxiliary *nor* the target task bear enough similarity with the pre-training task.

5 Discussion: towards updatable machine learning

In the grand scheme of things, we see model recycling within the emerging *updatable machine learning* [41] paradigm. The goal is to develop machine learning systems that can be incrementally improved and recombined, allowing for the collaborative creation of increasingly efficient and sophisticated AI systems. The core idea is to consider networks as pieces of software [67]; this enables mirroring open-source development in software engineering via version control. Could it be possible that, someday, we can collaboratively “clone”, “commit”, and “merge” models towards an ever-improving AI system?

Recent works [33, 34, 68, 69] and the proposed recycling give some primitives to build such a repository of neural networks. Here, (i) commits are fine-tunings performed by individual contributors on their specific tasks, and (ii) branch merging is replaced by weight averaging. In terms of optimization and privacy, a federated learning setup [70] where weights are communicated and averaged only at the end of the learning process does indeed seem desirable and viable [34, 71]. Moreover, advanced merging operations that consider weighted interpolations [33] or neuron permutations [72, 73, 74] could help. These ideas could lead to collaborative repositories where stakeholders open-source their fine-tuned models learned in a decentralized way on various auxiliary tasks [35, 58], all starting from a shared foundation model. This also opens the door to volunteer computing (SETI@home [75], Leela Chess Zero [76], etc), and even perhaps to remuneration incentives for contributors.

If this is the way forward, how can we ensure and maximize the *recyclability* of the resulting models? In software engineering, practices such as unit tests greatly reduce the failure modes of programs; how can we borrow these ideas to *specify and test* neural networks? To this end, we may leverage datasets as *test certificates* [77]. The community would monitor statistics such as accuracy, forgetting, fairness, and robustness against spurious correlations on these datasets. Then, the reported scores could guide the choice of what models to clone, fine-tune, and merge. However, bad actors could directly include these datasets in their training data; then, should these external datasets be watermarked [78], or kept secret by some certifying authority?

These questions are all the more important as traditional foundation models [1] come with centralization, monetization, data privacy issues, and lack of transparency [79]. Being able to collaboratively enrich weights opens the transition from *proprietary networks training* to *open-source collaborative networks building*. We see this as an exciting road ahead towards the responsible and reliable AI machine learning systems, that benefit us all.

References

- [1] Rishi Bommasani, Drew A Hudson, Ehsan Adeli, Russ Altman, Simran Arora, Sydney von Arx, Michael S Bernstein, Jeannette Bohg, Antoine Bosselut, Emma Brunskill, et al. On the opportunities and risks of foundation models. *arXiv preprint*, 2021. (pp. 1, 3, and 10)
- [2] Alex Fang, Gabriel Ilharco, Mitchell Wortsman, Yuhao Wan, Vaishaal Shankar, Achal Dave, and Ludwig Schmidt. Data determines distributional robustness in contrastive language image pre-training (CLIP). In *ICML*, 2022. (pp. 1 and 3)
- [3] Thao Nguyen, Gabriel Ilharco, Mitchell Wortsman, Sewoong Oh, and Ludwig Schmidt. Quality not quantity: On the interaction between dataset design and robustness of CLIP. In *NeurIPS*, 2022. (pp. 1 and 3)
- [4] Samira Abnar, Mostafa Dehghani, Behnam Neyshabur, and Hanie Sedghi. Exploring the limits of large scale pre-training. In *ICLR*, 2022. (p. 1)
- [5] Maxime Oquab, Leon Bottou, Ivan Laptev, and Josef Sivic. Learning and transferring mid-level image representations using convolutional neural networks. In *CVPR*, 2014. (pp. 1, 2, 3, and 18)
- [6] Andreas Christian Kirsch, Balaji Lakshminarayanan, Clara Huiyi Hu, D. Sculley, Du Phan, Dustin Tran, Jasper Roland Snoek, Jeremiah Liu, Jie Jessie Ren, Joost van Amersfoort, Kehang Han, Kelly Buchanan, Kevin Patrick Murphy, Mark Patrick Collier, Michael W. Dusenberry, Neil Band, Nithum Thain, Rodolphe Jenatton, Tim G. J. Rudner, Yarin Gal, Zachary Nado, Zelda Mariet, Zi Wang, and Zoubin Ghahramani. Plex: Towards reliability using pretrained large model extensions. In *ICML Workshop*, 2022. (p. 1)
- [7] Florian Wenzel, Andrea Dittadi, Peter Vincent Gehler, Carl-Johann Simon-Gabriel, Max Horn, Dominik Zietlow, David Kernert, Chris Russell, Thomas Brox, Bernt Schiele, Bernhard Schölkopf, and Francesco Locatello. Assaying out-of-distribution generalization in transfer learning. In *NeurIPS*, 2022. (pp. 1 and 17)
- [8] Sébastien Marcel and Yann Rodriguez. Torchvision the machine-vision package of torch. In *ACM*, 2010. (pp. 1, 2, and 3)
- [9] Thomas Wolf, Lysandre Debut, Victor Sanh, Julien Chaumond, Clement Delangue, Anthony Moi, Pierrick Cistac, Tim Rault, Remi Louf, Morgan Funtowicz, Joe Davison, Sam Shleifer, Patrick von Platen, Clara Ma, Yacine Jernite, Julien Plu, Canwen Xu, Teven Le Scao, Sylvain Gugger, Mariama Drame, Quentin Lhoest, and Alexander Rush. Transformers: State-of-the-art natural language processing. In *EMNLP*, 2020. (pp. 1, 2, and 3)
- [10] Martin Arjovsky, Léon Bottou, Ishaan Gulrajani, and David Lopez-Paz. Invariant risk minimization. *arXiv preprint*, 2019. (p. 1)
- [11] John Miller, Karl Krauth, Benjamin Recht, and Ludwig Schmidt. The effect of natural distribution shift on question answering models. In *ICML*, 2020. (p. 1)
- [12] Harshay Shah, Kaustav Tamuly, Aditi Raghunathan, Prateek Jain, and Praneeth Netrapalli. The pitfalls of simplicity bias in neural networks. In *NeurIPS*, 2020. (p. 1)
- [13] Shiori Sagawa, Pang Wei Koh, Tatsunori B. Hashimoto, and Percy Liang. Distributionally robust neural networks. In *ICLR*, 2020. (p. 1)

[14] Ishaan Gulrajani and David Lopez-Paz. In search of lost domain generalization. In *ICLR*, 2021. (pp. 1, 2, 3, 6, 7, 17, and 22)

[15] Dan Hendrycks and Thomas Dietterich. Benchmarking neural network robustness to common corruptions and perturbations. In *ICLR*, 2019. (p. 1)

[16] Dan Hendrycks, Steven Basart, Norman Mu, Saurav Kadavath, Frank Wang, Evan Dorundo, Rahul Desai, Tyler Zhu, Samyak Parajuli, Mike Guo, et al. The many faces of robustness: A critical analysis of out-of-distribution generalization. In *ICCV*, 2021. (p. 1)

[17] Rohan Taori, Achal Dave, Vaishaal Shankar, Nicholas Carlini, Benjamin Recht, and Ludwig Schmidt. Measuring robustness to natural distribution shifts in image classification. In *NeurIPS*, 2020. (p. 1)

[18] John R. Zech, Marcus A. Badgeley, Manway Liu, Anthony B. Costa, Joseph J. Titano, and Eric Karl Oermann. Variable generalization performance of a deep learning model to detect pneumonia in chest radiographs: A cross-sectional study. *PLoS Medicine*, 2018. (p. 1)

[19] Alexander D’Amour, Katherine Heller, Dan Moldovan, Ben Adlam, Babak Alipanahi, Alex Beutel, Christina Chen, Jonathan Deaton, Jacob Eisenstein, Matthew D Hoffman, et al. Underspecification presents challenges for credibility in modern machine learning. *JMLR*, 2020. (p. 1)

[20] Heang-Ping Chan, Lubomir M Hadjiiski, and Ravi K Samala. Computer-aided diagnosis in the era of deep learning. *Medical physics*, 2020. (p. 2)

[21] Alex J DeGrave, Joseph D Janizek, and Su-In Lee. AI for radiographic COVID-19 detection selects shortcuts over signal. *Nature Machine Intelligence*, 2021. (p. 2)

[22] Sampo Kuutti, Richard Bowden, Yaochu Jin, Phil Barber, and Saber Fallah. A survey of deep learning applications to autonomous vehicle control. *T-ITS*, 2020. (p. 2)

[23] Charles Corbière. Robust deep learning for autonomous driving. *arXiv preprint*, 2022. (p. 2)

[24] Ananya Kumar, Aditi Raghunathan, Robbie Matthew Jones, Tengyu Ma, and Percy Liang. Fine-tuning can distort pretrained features and underperform out-of-distribution. In *ICLR*, 2022. (pp. 2, 3, 5, 7, 9, and 22)

[25] Pavel Izmailov, Dmitrii Podoprikhin, Timur Garipov, Dmitry Vetrov, and Andrew Gordon Wilson. Averaging weights leads to wider optima and better generalization. In *UAI*, 2018. (pp. 2, 3, 17, and 18)

[26] Behnam Neyshabur, Hanie Sedghi, and Chiyuan Zhang. What is being transferred in transfer learning? In *NeurIPS*, 2020. (pp. 2 and 4)

[27] Devansh Arpit, Huan Wang, Yingbo Zhou, and Caiming Xiong. Ensemble of averages: Improving model selection and boosting performance in domain generalization. In *NeurIPS*, 2021. (pp. 2, 4, 7, 22, 23, and 24)

[28] Mitchell Wortsman, Gabriel Ilharco, Jong Wook Kim, Mike Li, Hanna Hajishirzi, Ali Farhadi, Hongseok Namkoong, and Ludwig Schmidt. Robust fine-tuning of zero-shot models. In *CVPR*, 2022. (pp. 2, 4, 6, and 18)

[29] Mitchell Wortsman, Gabriel Ilharco, Samir Yitzhak Gadre, Rebecca Roelofs, Raphael Gontijo-Lopes, Ari S. Morcos, Hongseok Namkoong, Ali Farhadi, Yair Carmon, Simon Kornblith, and Ludwig Schmidt. Model soups: averaging weights of multiple fine-tuned models improves accuracy without increasing inference time. In *ICML*, 2022. (pp. 2, 4, 5, 6, 7, 8, 17, and 18)

[30] Alexandre Rame, Matthieu Kirchmeyer, Thibaud Rahier, Alain Rakotomamonjy, Patrick Gallinari, and Matthieu Cord. Diverse weight averaging for out-of-distribution generalization. In *NeurIPS*, 2022. (pp. 2, 4, 5, 6, 7, 8, 17, 18, 22, 23, and 24)

[31] Jason Phang, Thibault Févry, and Samuel R Bowman. Sentence encoders on stilts: Supplementary training on intermediate labeled-data tasks. *arXiv preprint*, 2018. (pp. 2, 4, 6, 7, 18, 23, and 24)

[32] Yada Pruksachatkun, Jason Phang, Haokun Liu, Phu Mon Htut, Xiaoyi Zhang, Richard Yuanzhe Pang, Clara Vania, Katharina Kann, and Samuel Bowman. Intermediate-task transfer learning with pretrained language models: When and why does it work? In *ACL*, 2020. (pp. 2 and 4)

[33] Michael Matena and Colin Raffel. Merging models with Fisher-weighted averaging. In *NeurIPS*, 2022. (pp. 2, 3, 4, and 10)

[34] Margaret Li, Suchin Gururangan, Tim Dettmers, Mike Lewis, Tim Althoff, Noah A Smith, and Luke Zettlemoyer. Branch-Train-Merge: Embarrassingly parallel training of expert language models. *arXiv preprint*, 2022. (pp. 2, 3, 4, 6, 9, 10, and 18)

[35] Leshem Choshen, Elad Venezian, Noam Slonim, and Yoav Katz. Fusing finetuned models for better pretraining. *arXiv preprint*, 2022. (pp. 2, 4, 6, 7, 10, 18, 23, and 24)

[36] Firas Laakom, Jenni Raitoharju, Alexandros Iosifidis, and Moncef Gabbouj. Within-layer diversity reduces generalization gap. In *ICML Workshop*, 2021. (pp. 2 and 6)

[37] Niv Nayman, Avram Golbert, Asaf Noy, Tan Ping, and Lihi Zelnik-Manor. Diverse ImageNet models transfer better. *arXiv preprint*, 2022. (pp. 2 and 6)

[38] Saachi Jain, Dimitris Tsipras, and Aleksander Madry. Combining diverse feature priors. In *ICML*, 2022. (pp. 2, 6, and 8)

[39] Jianyu Zhang, David Lopez-Paz, and Léon Bottou. Rich feature construction for the optimization-generalization dilemma. In *ICML*, 2022. (pp. 2, 4, 6, and 8)

[40] Jianyu Zhang and Léon Bottou. Learning useful representations for shifting tasks and distributions. *arXiv preprint*, 2022. (pp. 2, 4, and 6)

[41] Colin Raffel. A call to build models like we build open-source software. <https://colinraffel.com/blog/a-call-to-build-models-like-we-build-open-source-software.html>. Accessed: 2022-12-19. (pp. 3 and 10)

[42] V. Vapnik. Principles of risk minimization for learning theory. In *NeurIPS*, 1992. (p. 3)

[43] Olga Russakovsky, Jia Deng, Hao Su, Jonathan Krause, Sanjeev Satheesh, Sean Ma, Zhiheng Huang, Andrej Karpathy, Aditya Khosla, Michael Bernstein, et al. ImageNet large scale visual recognition challenge. In *IJCV*, 2015. (pp. 3 and 7)

[44] Da Li, Yongxin Yang, Yi-Zhe Song, and Timothy M Hospedales. Deeper, broader and artier domain generalization. In *ICCV*, 2017. (pp. 3, 6, and 22)

[45] Chen Fang, Ye Xu, and Daniel N Rockmore. Unbiased metric learning: On the utilization of multiple datasets and web images for softening bias. In *ICCV*, 2013. (pp. 3, 6, and 22)

[46] Hemanth Venkateswara, Jose Eusebio, Shayok Chakraborty, and Sethuraman Panchanathan. Deep hashing network for unsupervised domain adaptation. In *CVPR*, 2017. (pp. 3, 6, and 22)

[47] Sara Beery, Grant Van Horn, and Pietro Perona. Recognition in Terra Incognita. In *ECCV*, 2018. (pp. 3, 6, and 22)

[48] Xingchao Peng, Qinxun Bai, Xide Xia, Zijun Huang, Kate Saenko, and Bo Wang. Moment matching for multi-source domain adaptation. In *ICCV*, 2019. (pp. 3, 6, and 22)

[49] Priya Goyal, Quentin Duval, Isaac Seessel, Mathilde Caron, Mannat Singh, Ishan Misra, Levent Sagun, Armand Joulin, and Piotr Bojanowski. Vision models are more robust and fair when pretrained on uncurated images without supervision. *arXiv preprint*, 2022. (p. 3)

[50] Felix Draxler, Kambis Veschgini, Manfred Salmhofer, and Fred Hamprecht. Essentially no barriers in neural network energy landscape. In *ICML*, 2018. (p. 3)

[51] Jonathan Frankle, Gintare Karolina Dziugaite, Daniel M. Roy, and Michael Carbin. Linear mode connectivity and the lottery ticket hypothesis. In *ICML*, 2020. (pp. 3 and 4)

[52] Junbum Cha, Sanghyuk Chun, Kyungjae Lee, Han-Cheol Cho, Seunghyun Park, Yunsung Lee, and Sungrae Park. SWAD: Domain generalization by seeking flat minima. In *NeurIPS*, 2021. (pp. 4, 7, 22, 23, and 24)

[53] Ludmila I Kuncheva and Christopher J Whitaker. Measures of diversity in classifier ensembles and their relationship with the ensemble accuracy. *Machine learning*, 2003. (pp. 4, 8, 18, and 19)

[54] Matti Aksela. Comparison of classifier selection methods for improving committee performance. In *MCS*, 2003. (pp. 4, 8, and 19)

[55] Balaji Lakshminarayanan, Alexander Pritzel, and Charles Blundell. Simple and scalable predictive uncertainty estimation using deep ensembles. In *NeurIPS*, 2017. (pp. 4 and 7)

[56] Ting-Yun Chang and Chi-Jen Lu. Rethinking why intermediate-task fine-tuning works. *arXiv preprint*, 2021. (pp. 4 and 8)

[57] Sylvestre-Alvise Rebuffi, Alexander Kolesnikov, Georg Sperl, and Christoph H Lampert. iCaRL: Incremental classifier and representation learning. In *CVPR*, 2017. (p. 4)

[58] Shachar Don-Yehiya, Elad Venezian, Colin Raffel, Noam Slonim, Yoav Katz, and Leshem Choshen. ColD fusion: Collaborative descent for distributed multitask finetuning. *arXiv preprint*, 2022. (pp. 6 and 10)

[59] Leshem Choshen, Elad Venezian, Shachar Don-Yehia, Noam Slonim, and Yoav Katz. Where to start? analyzing the potential value of intermediate models. *arXiv preprint*, 2022. (p. 6)

[60] Gabriel Ilharco, Mitchell Wortsman, Samir Yitzhak Gadre, Shuran Song, Hannaneh Hajishirzi, Simon Kornblith, Ali Farhadi, and Ludwig Schmidt. Patching open-vocabulary models by interpolating weights. In *NeurIPS*, 2022. (p. 6)

[61] Baochen Sun, Jiashi Feng, and Kate Saenko. Return of frustratingly easy domain adaptation. In *AAAI*, 2016. (pp. 7, 22, 23, and 24)

[62] Kaiming He, Xiangyu Zhang, Shaoqing Ren, and Jian Sun. Deep residual learning for image recognition. In *CVPR*, 2016. (pp. 7 and 22)

[63] Raphael Gontijo-Lopes, Yann Dauphin, and Ekin Dogus Cubuk. No one representation to rule them all: Overlapping features of training methods. In *ICLR*, 2022. (p. 8)

[64] J Taylor, B Earnshaw, B Mabey, M Victors, and J Yosinski. RxRx1: An image set for cellular morphological variation across many experimental batches. In *ICLR*, 2019. (p. 9)

[65] Pang Wei Koh, Shiori Sagawa, Henrik Marklund, Sang Michael Xie, Marvin Zhang, Akshay Balsubramani, Weihua Hu, Michihiro Yasunaga, Richard Lanas Phillips, Irena Gao, Tony Lee, Etienne David, Ian Stavness, Wei Guo, Berton Earnshaw, Imran Haque, Sara M Beery, Jure Leskovec, Anshul Kundaje, Emma Pierson, Sergey Levine, Chelsea Finn, and Percy Liang. WILDS: A benchmark of in-the-wild distribution shifts. In *ICML*, 2021. (p. 9)

[66] Yujia Qin, Cheng Qian, Jing Yi, Weize Chen, Yankai Lin, Xu Han, Zhiyuan Liu, Maosong Sun, and Jie Zhou. Exploring mode connectivity for pre-trained language models. In *EMNLP*, 2022. (p. 9)

[67] Andrej Karpathy. Software 2.0. <https://karpathy.medium.com/software-2-0-a64152b37c35>, 2017. Accessed: 2022-12-19. (p. 10)

[68] Gabriel Ilharco, Marco Tulio Ribeiro, Mitchell Wortsman, Suchin Gururangan, Ludwig Schmidt, Hannaneh Hajishirzi, and Ali Farhadi. Editing models with task arithmetic. *arXiv preprint*, 2022. (p. 10)

[69] Alexander Borzunov, Dmitry Baranchuk, Tim Dettmers, Max Ryabinin, Younes Belkada, Artem Chumachenko, Pavel Samygin, and Colin Raffel. Petals: Collaborative inference and fine-tuning of large models. *arXiv preprint*, 2022. (p. 10)

[70] Qinbin Li, Zeyi Wen, and Bingsheng He. Federated learning systems: Vision, hype and reality for data privacy and protection. *arXiv preprint*, 2019. (p. 10)

[71] Mitchell Wortsman, Suchin Gururangan, Shen Li, Ali Farhadi, Ludwig Schmidt, Michael Rabbat, and Ari S Morcos. lo-fi: distributed fine-tuning without communication. *arXiv preprint*, 2022. (p. 10)

[72] Rahim Entezari, Hanie Sedghi, Olga Saukh, and Behnam Neyshabur. The role of permutation invariance in linear mode connectivity of neural networks. In *ICLR*, 2022. (p. 10)

[73] Samuel K. Ainsworth, Jonathan Hayase, and Siddhartha Srinivasa. Git re-basin: Merging models modulo permutation symmetries. *arXiv preprint*, 2022. (p. 10)

[74] Keller Jordan, Hanie Sedghi, Olga Saukh, Rahim Entezari, and Behnam Neyshabur. Repair: Renormalizing permuted activations for interpolation repair. *arXiv preprint*, 2022. (p. 10)

[75] Dustin Anderson, Jeff Cobb, Eric J. Korpela, Matt Lebofsky, and Dan Werthimer. SETI@home: an experiment in public-resource computing. *ACM*, 2002. (p. 10)

[76] Pascutto, Gian-Carlo and Linscott, Gary. Leela Chess Zero. <http://lczero.org/>. (p. 10)

[77] David Lopez-Paz, Diane Bouchacourt, Levent Sagun, and Nicolas Usunier. Measuring and signing fairness as performance under multiple stakeholder distributions. *arXiv preprint*, 2022. (p. 10)

- [78] Yue Li, Hongxia Wang, and Mauro Barni. A survey of deep neural network watermarking techniques. *Neurocomputing*, 2021. (p. 10)
- [79] Rishi Bommasani and Percy Liang. Reflections on foundation models. <https://hai.stanford.edu/news/reflections-foundation-models>. Accessed: 2022-12-19. (p. 10)
- [80] Arthur Jacot, Franck Gabriel, and Clement Hongler. Neural tangent kernel: Convergence and generalization in neural networks. In *NeurIPS*, 2018. (p. 17)
- [81] Damien Teney, Yong Lin, Seong Joon Oh, and Ehsan Abbasnejad. ID and OOD performance are sometimes inversely correlated on real-world datasets. *arXiv preprint*, 2022. (p. 17)
- [82] John P Miller, Rohan Taori, Aditi Raghunathan, Shiori Sagawa, Pang Wei Koh, Vaishaal Shankar, Percy Liang, Yair Carmon, and Ludwig Schmidt. Accuracy on the line: on the strong correlation between out-of-distribution and in-distribution generalization. In *ICML*, 2021. (p. 17)
- [83] George Udny Yule. On the association of attributes in statistics. *Philosophical Transactions of the Royal Society of London.*, 1900. (p. 18)
- [84] Alexandre Rame and Matthieu Cord. DICE: Diversity in deep ensembles via conditional redundancy adversarial estimation. In *ICLR*, 2021. (pp. 18 and 19)
- [85] Diederik P. Kingma and Jimmy Ba. Adam: A method for stochastic optimization. In *ICLR*, 2015. (p. 22)
- [86] Jonas Peters, Peter Bühlmann, and Nicolai Meinshausen. Causal inference by using invariant prediction: identification and confidence intervals. *JSTOR*, 2016. (p. 22)

Recycling diverse models for out-of-distribution generalization

Supplementary material

This supplementary material is organized as follows:

- Appendix A discusses the interest of recycling for ID tasks.
- Appendix B describes the different fine-tuning strategies with pseudo-equations.
- Appendix C clarifies our diversity measures.
- Appendix D further empirically analyzes the validity of Hypothesis 2.
- Appendix E describes our experimental setup on DomainBed [14].

A Recycling for ID tasks

Like previous weight averaging strategies [25, 29], recycling also works for ID tasks, yet with smaller gains than in OOD. This is what we validate in Figure 5, where the LMC usually holds in ID (when RxRx is not the auxiliary task), yet with curves less concave than in OOD. These smaller gains when interpolating is because variance reduction via weight averaging is less beneficial in ID than in OOD. Theoretically, this is because, as explained in [30] in the NTK [80] regime, variance is smaller without distribution shift. Empirically, this is consistent with the fact that models’ diversity is smaller in ID, as shown in Figure 6a. Overall, diversity procedures (like recycling) are less useful in ID than in OOD. The conclusion is a lack of correlation between ID and OOD accuracies [81], as shown in Figures 6b and 6c. This finding contrasts with recent works [7, 82] and goes against the prescription in [7] that, “to make the model more robust on OOD data, the main focus should be to improve the ID classification error”.

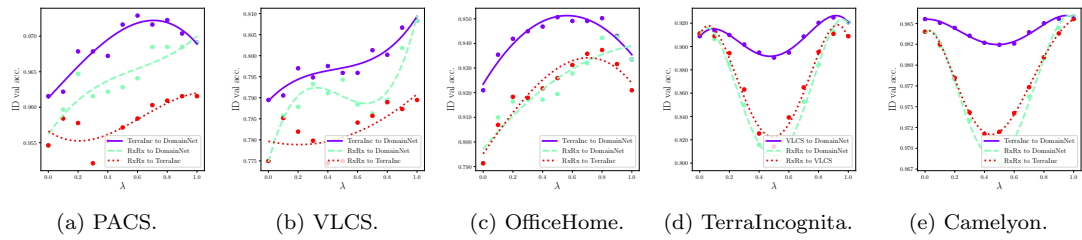


Figure 5: Empirical analysis of Hypothesis 2 on the ID validation split of the training domains. These Figures 5a to 5e mirror the setup from Figures 4f to 4j.

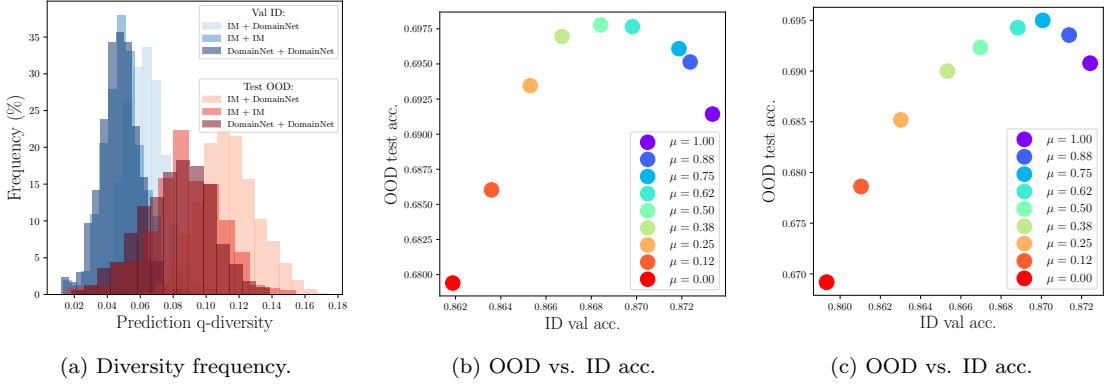


Figure 6: Relations between diversity, ID and OOD accuracies. The models were trained on ID domains “Clipart,Product,Photo” from OfficeHome, thus “Art” is the OOD domain. In (a), we compute the diversity [53] between models either directly fine-tuned from ImageNet, either inter-trained on DomainNet. Though having different initializations increases diversity both in ID and in OOD, the diversity in ID remains smaller. In (b), we report the mean results when averaging $M = 8$ weights: $(1 - \mu)$ are fine-tuned on OfficeHome directly from ImageNet, the others μ are inter-trained on DomainNet. We observe a lack of correlation between ID and OOD accuracies in (b), but also in (c), where the proportion $(1 - \mu)$ are inter-trained on PACS.

B Fine-tuning strategies as pseudo-equations

In Figure 1, we illustrated the different fine-tuning strategies. In Equation (1), we now provide an analytical formulation of these strategies with pseudo-equations, where θ represents the weights, A_i the auxiliary tasks and T the target task.

$$\begin{aligned}
 \theta &= \text{Train}(\theta^{\text{pt}}, T), & & [\text{Vanilla fine-tuning [5]}] \\
 \theta &= \text{Train}(\theta^{\text{pt}}, T, \text{collect_ckpts} = \text{True}), & & [\text{Moving average [25]}] \\
 \theta &= (1 - \lambda) \cdot \text{Train}(\theta^{\text{pt}}, T) + \lambda \cdot \theta^{\text{pt}}, & & [\text{WiSE fine-tuning [28]}] \\
 \theta &= \frac{1}{M} \sum_{i=1}^M \text{Train}(\theta^{\text{pt}}, T), & & [\text{Model Soups [29]/DiWA [30]}] \\
 \theta &= \text{Train}(\text{Train}(\theta^{\text{pt}}, A_i), T), & & [\text{Inter-training [31]}] \\
 \theta &= \text{Train}\left(\sum_i \kappa_i \cdot \text{Train}(\theta^{\text{pt}}, A_i), T\right), & & [\text{Fusing [34, 35]}] \\
 \theta &= \frac{1}{M} \sum_{i=1}^M \text{Train}(\text{Train}(\theta^{\text{pt}}, A_i), T), & & [\text{Recycling (ours)}]
 \end{aligned} \tag{1}$$

C Diversity measures

As stated in “Measures of Diversity in Classifier Ensembles and Their Relationship with the Ensemble Accuracy” [53], “measuring diversity is not straightforward because there is no generally accepted formal definition”. In Figure 3, we leverage the q-statistics Q , introduced in Yule [83], brought up to date in [53] and also used in [84]. Specifically, it is defined by $Q = \frac{N^{11}N^{00} - N^{01}N^{10}}{N^{11}N^{00} + N^{01}N^{10}}$, where N^{ij} is the number of times that the first classifier is (correct if $i = 1$ or wrong if $i = 0$) and

the second classifier is (correct if $j = 1$ or wrong if $j = 0$). For example, N^{10} is the number of times that the first classifier is correct but not the second. Overall, classifiers which commit errors on different objects will render Q small. To transform this similarity into a diversity measure that increases for more diverse classifiers, we report 1 minus the q-statistics, i.e., $1 - Q$.

In Figure 7, we measure diversity with another diversity measure, the ratio-error, introduced in [54] (\uparrow), brought up to date in [53] and also used in [84]. This ratio-error is the ratio $\frac{N^{01} + N^{10}}{N^{00}}$ between the number of asynchronous errors and of simultaneous errors for two classifiers. This r-diversity leads to similar conclusions as with the q-diversity.

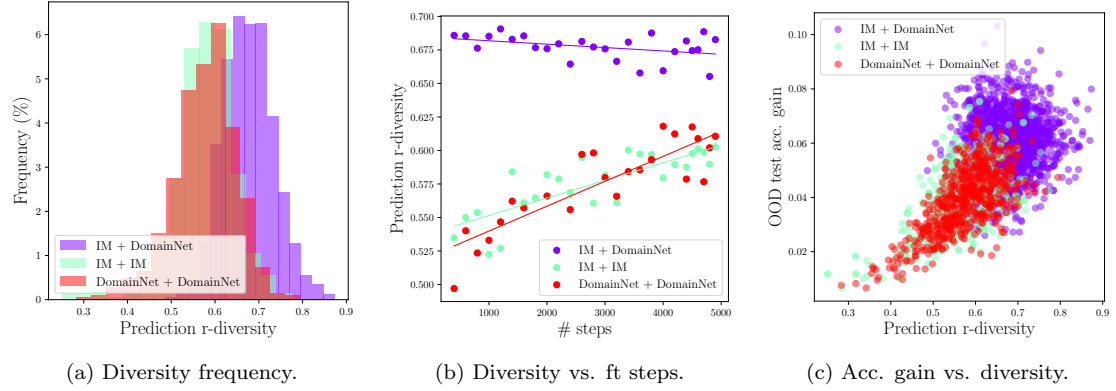


Figure 7: We reproduce Figure 3 leveraging the ratio-error [54] r-diversity measure.

D Linear mode connectivity experiments

We further empirically analyze our Hypothesis 2. In particular, we observe that the LMC usually holds except in two cases. First, when the OOD test domain is the “LabelMe” domain from VLCS (in Figure 9b from Appendix D). Second, when both the target and the auxiliary tasks are distant from the pre-trained task, for example when tackling TerraIncognita or Camelyon with RxRx as an auxiliary task. We want to emphasize that we selected the “extreme” RxRx dataset precisely to test the empirical limits of the Hypothesis 2, but that, in practice, milder auxiliary tasks selection already helps for OOD generalization (see Section 4.1).

D.1 PACS

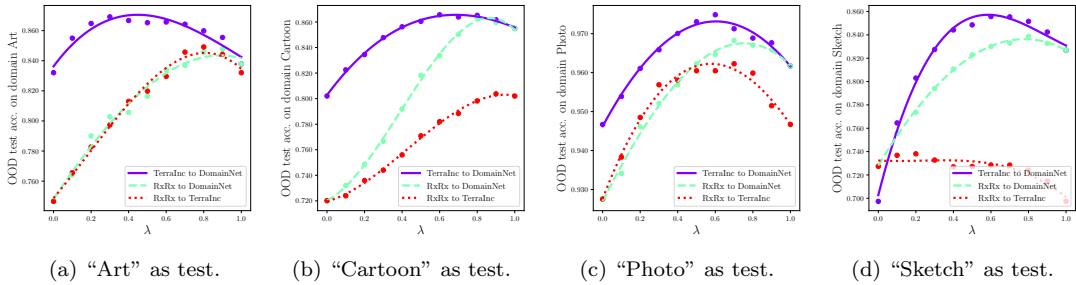


Figure 8: Empirical analysis of Hypothesis 2 on PACS.

D.2 VLCS

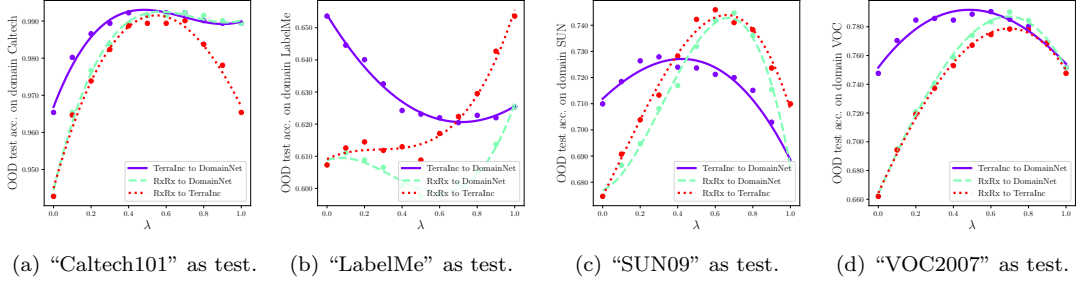


Figure 9: Empirical analysis of Hypothesis 2 on VLCS.

D.3 OfficeHome

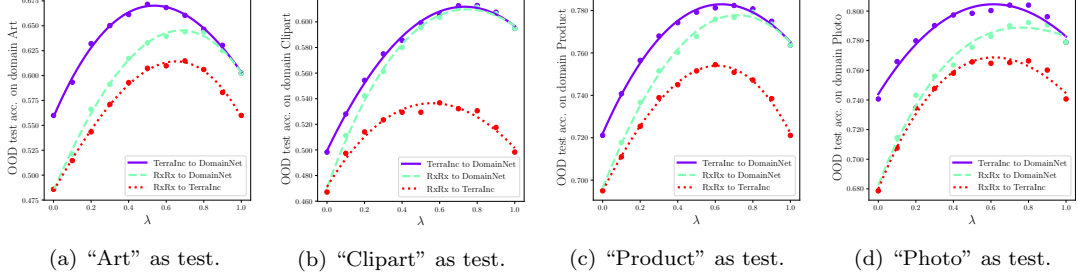


Figure 10: Empirical analysis of Hypothesis 2 on OfficeHome.

D.4 TerraIncognita

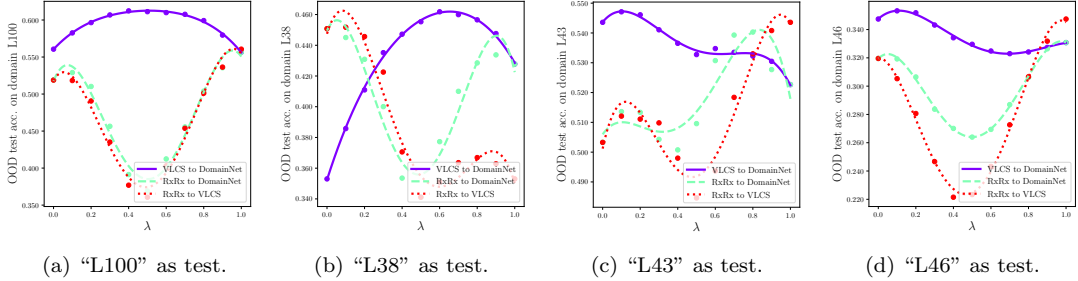


Figure 11: Empirical analysis of Hypothesis 2 on TerraIncognita.

D.5 Camelyon

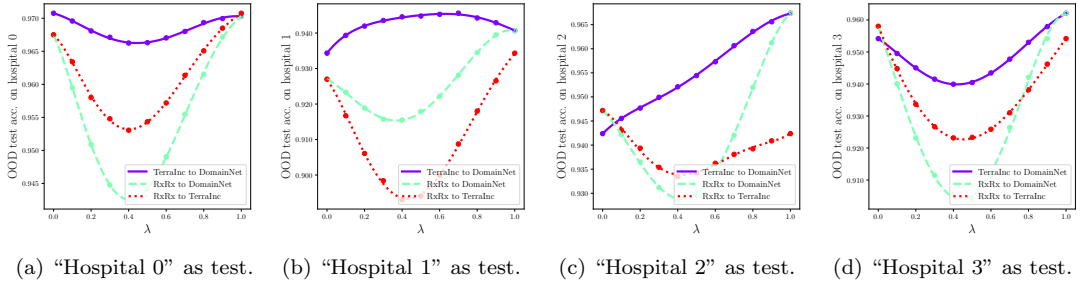


Figure 12: Empirical analysis of Hypothesis 2 on Camelyon.

D.6 Recycling of weights fine-tuned sequentially on multiple datasets

In Figure 13, we empirically analyze Hypothesis 2 when the intermediate tasks are themselves several successive trainings on different auxiliary datasets. Therefore the initialization for “TerraInc.VLCS” in the purple line of Figure 13c was sequentially fine-tuned on two auxiliary tasks (TerraIncognita and then on VLCS) before fine-tuning on the target task (OfficeHome). The concavity of the curves validates the LMC in this setup. It hints towards a more general inheritance property of LMC: if two initializations satisfy the LMC, then the two fine-tuned weights too. Yet, full analysis of this inheritance property is best left for future work.

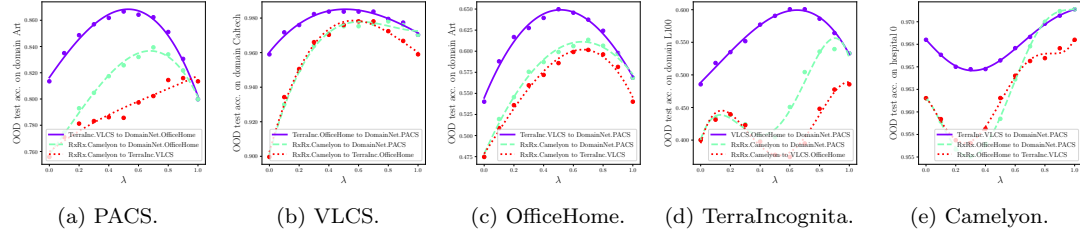


Figure 13: Empirical analysis of Hypothesis 2 when the intermediate tasks are themselves several successive fine-tunings on different auxiliary datasets. “Dataset_a.Dataset_b to Dataset_c.Dataset_d” means that the model for $\lambda = 0$ was sequentially fine-tuned on Dataset_a then Dataset_b before fine-tuning on the target task, while the model for $\lambda = 1$ was sequentially fine-tuned on Dataset_c then Dataset_d before fine-tuning on the target task; $0 < \lambda < 1$ interpolates between those two fine-tuned weights. Following Section 4.3, on each target task, we consider the first domain as the test OOD domain.

E DomainBed

We further detail our experiments on the DomainBed benchmark [14].

E.1 Experimental details

Training protocol. We leverage the PACS [44], VLCS [45], OfficeHome [46], TerraIncognita [47] and DomainNet [48] datasets. Domains are split into 80% (used as training and evaluation) and 20% (used as validation). When considered as the target task, each domain is successively considered as the test domain while others are for training. When considered as an auxiliary task, we train on all domains simultaneously. We follow the training protocol from DomainBed. For each dataset and domain, we perform a random search of 20 trials on the mild hyperparameter distributions described in Table 2. We use a ResNet-50 [62] pre-trained on ImageNet, with a dropout layer before the newly added dense layer and fine-tuned with frozen batch normalization layers. The optimizer is Adam [85]. The linear probe classifier are obtained with default hyperparameters from Table 2 and features extracted from the ImageNet pre-trained featurizer. All runs are trained for 5k steps, except on DomainNet with 15k steps as done in concurrent works [27, 30, 52]. When the featurizer was inter-trained on auxiliary datasets, it remains frozen during the first 200 steps to prevent feature distortion [24]. As in [30, 52], validation accuracy is calculated every 50 steps for VLCS, 500 steps for DomainNet and 100 steps for others. Our code will be released at <https://github.com/facebookresearch/ModelRecycling>.

Baselines. ERM is the vanilla fine-tuning with standard Empirical Risk Minimization. CORAL [61] is the best invariance-based [86] approach. The vanilla scores for ERM and CORAL are taken from DomainBed [14]. MA [27] and SWAD [52] average weights along the trajectory of an ERM run; their scores are taken from their respective papers. Deep ensembles* [27] averages the predictions of $M = 6$ models, each trained with different classifier initializations on different data splits. DiWA [30] averages the weights obtained from different ERM runs; for fair comparison, we report the scores DiWA achieved with linear probing. Fusing averages multiple auxiliary weights but at initialization; for each of the 20 runs, we sample $\{\kappa_i\}_{i=1}^5 \sim \text{Unif}(0, 4)$, and start training from $\sum_{i=1}^5 \frac{e^{\kappa_i}}{\sum_{j=1}^5 e^{\kappa_j}} \phi_i^{\text{aux}}$.

Model and weight selection. We consider the training-domain validation set protocol. From each run, we thus take the weights at the epoch with maximum accuracy on the ID validation dataset. The greedy weight selection is also based on this ID validation set. This greedy strategy is not possible for \dagger approaches, that average uniformly the $M = 20 \times 3 = 60$ weights from the 3 data splits: indeed, there is no shared ID validation dataset.

Table 2: Hyperparameters, their default values and distributions for random search.

Hyperparameter	Default value	Random distribution	
		Extreme (DomainBed)	Mild (Ours, DiWA and SWAD)
Learning rate	$5 \cdot 10^{-5}$	$10^{\mathcal{U}(-5, -3.5)}$	$[1, 3, 5] \cdot 10^{-5}$
Batch size	32	$2^{\mathcal{U}(3, 5.5)}$	32
ResNet dropout	0	$[0, 0.1, 0.5]$	$[0, 0.1, 0.5]$
Weight decay	0	$10^{\mathcal{U}(-6, -2)}$	$[10^{-6}, 10^{-4}]$

E.2 Results per dataset

Table 3: Accuracy (%,\$\uparrow\$) on PACS (best in **bold** and second underlined).

Algorithm	Selection	Art	Cartoon	Photo	Sketch	Avg	
ERM	ID val	84.7 \$\pm\$ 0.4	80.8 \$\pm\$ 0.6	97.2 \$\pm\$ 0.3	79.3 \$\pm\$ 1.0	85.5 \$\pm\$ 0.2	
CORAL [61]	ID val	88.3 \$\pm\$ 0.2	80.0 \$\pm\$ 0.5	97.5 \$\pm\$ 0.3	78.8 \$\pm\$ 1.3	86.2 \$\pm\$ 0.3	
SWAD [52]	Loss-aware trajectory	89.3 \$\pm\$ 0.5	83.4 \$\pm\$ 0.6	97.3 \$\pm\$ 0.3	82.5 \$\pm\$ 0.8	88.1 \$\pm\$ 0.1	
MA [27]	Uniform trajectory	89.1 \$\pm\$ 0.1	82.6 \$\pm\$ 0.2	97.6 \$\pm\$ 0.0	80.5 \$\pm\$ 0.9	87.5 \$\pm\$ 0.2	
Deep ensembles* [27]	Uniform	88.3	83.6	96.5	81.9	87.6	
DiWA[30] runs	ERM	86.8 \$\pm\$ 0.8	80.6 \$\pm\$ 1.0	97.4 \$\pm\$ 0.4	78.7 \$\pm\$ 2.0	85.9 \$\pm\$ 0.6	
	Ensemble*	89.6 \$\pm\$ 0.2	81.6 \$\pm\$ 0.3	97.8 \$\pm\$ 0.2	83.5 \$\pm\$ 0.5	88.1 \$\pm\$ 0.3	
	Model Soups/DiWA	90.1 \$\pm\$ 0.2	82.8 \$\pm\$ 0.6	98.3 \$\pm\$ 0.1	83.3 \$\pm\$ 0.4	88.7 \$\pm\$ 0.2	
	Model Soups/DiWA	89.3 \$\pm\$ 0.2	82.8 \$\pm\$ 0.2	98.0 \$\pm\$ 0.1	82.0 \$\pm\$ 0.9	88.0 \$\pm\$ 0.3	
	Model Soups/DiWA [†]	90.6	83.4	98.2	83.8	89.0	
Our runs	Inter-training [31]	ID val	89.2 \$\pm\$ 1.0	85.3 \$\pm\$ 0.7	97.5 \$\pm\$ 0.0	84.2 \$\pm\$ 0.2	89.0 \$\pm\$ 0.0
	Ensemble* of inter-training	Uniform	90.4 \$\pm\$ 0.2	83.7 \$\pm\$ 0.3	97.9 \$\pm\$ 0.2	84.9 \$\pm\$ 0.3	89.2 \$\pm\$ 0.1
	Fusing [35]	ID val	90.8 \$\pm\$ 0.1	79.1 \$\pm\$ 1.4	98.0 \$\pm\$ 0.4	84.1 \$\pm\$ 2.1	88.0 \$\pm\$ 1.0
	Recycling	Uniform	90.3 \$\pm\$ 0.2	84.4 \$\pm\$ 0.1	98.7 \$\pm\$ 0.1	84.8 \$\pm\$ 0.1	89.5 \$\pm\$ 0.1
	Recycling	Greedy	90.9 \$\pm\$ 0.1	86.5 \$\pm\$ 1.1	98.6 \$\pm\$ 0.0	85.9 \$\pm\$ 0.4	90.5 \$\pm\$ 0.2
	Recycling [†]	Uniform [†]	90.6	84.7	98.8	85.0	89.8

Table 4: Accuracy (%,\$\uparrow\$) on VLCS (best in **bold** and second underlined).

Algorithm	Selection	Caltech	LabelMe	SUN	VOC	Avg	
ERM	ID val	97.7 \$\pm\$ 0.4	64.3 \$\pm\$ 0.9	73.4 \$\pm\$ 0.5	74.6 \$\pm\$ 1.3	77.5 \$\pm\$ 0.4	
CORAL [61]	ID val	98.3 \$\pm\$ 0.1	66.1 \$\pm\$ 1.2	73.4 \$\pm\$ 0.3	77.5 \$\pm\$ 1.2	78.8 \$\pm\$ 0.6	
SWAD [52]	Loss-aware trajectory	98.8 \$\pm\$ 0.1	63.3 \$\pm\$ 0.3	75.3 \$\pm\$ 0.5	79.2 \$\pm\$ 0.6	79.1 \$\pm\$ 0.1	
MA [27]	Uniform trajectory	99.0 \$\pm\$ 0.2	63.0 \$\pm\$ 0.2	<u>74.5</u> \$\pm\$ 0.3	76.4 \$\pm\$ 1.1	78.2 \$\pm\$ 0.2	
Deep ensembles* [27]	Uniform	98.7	64.5	72.1	78.9	78.5	
DiWA[30] runs	ERM	98.1 \$\pm\$ 0.3	64.4 \$\pm\$ 0.3	72.5 \$\pm\$ 0.5	77.7 \$\pm\$ 1.3	78.1 \$\pm\$ 0.5	
	Ensemble*	98.5 \$\pm\$ 0.1	<u>64.9</u> \$\pm\$ 0.1	73.4 \$\pm\$ 0.4	77.2 \$\pm\$ 0.4	78.5 \$\pm\$ 0.1	
	Model Soups/DiWA	98.8 \$\pm\$ 0.1	62.8 \$\pm\$ 0.2	73.9 \$\pm\$ 0.3	78.3 \$\pm\$ 0.1	78.4 \$\pm\$ 0.2	
	Model Soups/DiWA	98.4 \$\pm\$ 0.0	64.1 \$\pm\$ 0.2	73.3 \$\pm\$ 0.4	78.1 \$\pm\$ 0.8	78.5 \$\pm\$ 0.1	
	Model Soups/DiWA [†]	98.9	62.4	73.9	78.9	78.6	
Our runs	Inter-training [31]	ID val	98.2 \$\pm\$ 0.0	63.8 \$\pm\$ 0.5	72.3 \$\pm\$ 0.5	76.6 \$\pm\$ 0.2	77.7 \$\pm\$ 0.0
	Ensemble* of inter-training	Uniform	98.9 \$\pm\$ 0.1	<u>64.7</u> \$\pm\$ 0.4	73.8 \$\pm\$ 0.5	78.6 \$\pm\$ 0.2	<u>79.0</u> \$\pm\$ 0.2
	Fusing [35]	ID val	98.4 \$\pm\$ 0.4	64.8 \$\pm\$ 1.2	72.2 \$\pm\$ 0.9	78.5 \$\pm\$ 0.6	78.5 \$\pm\$ 0.8
	Recycling	Uniform	99.3 \$\pm\$ 0.0	60.8 \$\pm\$ 0.3	74.3 \$\pm\$ 0.3	79.5 \$\pm\$ 0.3	78.5 \$\pm\$ 0.1
	Recycling	Greedy	99.0 \$\pm\$ 0.0	62.4 \$\pm\$ 0.5	73.8 \$\pm\$ 0.3	79.5 \$\pm\$ 0.1	78.7 \$\pm\$ 0.2
	Recycling [†]	Uniform [†]	99.3	60.4	73.9	79.5	78.3

Table 5: Accuracy (%,\$\uparrow\$) on OfficeHome (best in **bold** and second underlined).

Algorithm	Selection	Art	Clipart	Product	Photo	Avg
ERM	ID val	61.3 \$\pm\$ 0.7	52.4 \$\pm\$ 0.3	75.8 \$\pm\$ 0.1	76.6 \$\pm\$ 0.3	66.5 \$\pm\$ 0.3
CORAL [61]	ID val	65.3 \$\pm\$ 0.4	54.4 \$\pm\$ 0.5	76.5 \$\pm\$ 0.1	78.4 \$\pm\$ 0.5	68.7 \$\pm\$ 0.3
SWAD [52]	Loss-aware trajectory	66.1 \$\pm\$ 0.4	57.7 \$\pm\$ 0.4	78.4 \$\pm\$ 0.1	80.2 \$\pm\$ 0.2	70.6 \$\pm\$ 0.2
MA [27]	Uniform trajectory	66.7 \$\pm\$ 0.5	57.1 \$\pm\$ 0.1	78.6 \$\pm\$ 0.1	80.0 \$\pm\$ 0.0	70.6 \$\pm\$ 0.1
Deep ensembles* [27]	Uniform	65.6	58.5	78.7	80.5	70.8
DiWA[30] runs	ERM	63.9 \$\pm\$ 1.2	54.8 \$\pm\$ 0.6	78.7 \$\pm\$ 0.1	80.4 \$\pm\$ 0.2	69.4 \$\pm\$ 0.2
	Ensemble*	67.0 \$\pm\$ 0.1	57.9 \$\pm\$ 0.4	80.0 \$\pm\$ 0.2	81.7 \$\pm\$ 0.3	71.7 \$\pm\$ 0.1
	Model Soups/DiWA	68.4 \$\pm\$ 0.2	58.2 \$\pm\$ 0.5	80.0 \$\pm\$ 0.1	81.7 \$\pm\$ 0.3	72.1 \$\pm\$ 0.2
	Model Soups/DiWA	67.8 \$\pm\$ 0.5	57.2 \$\pm\$ 0.5	79.6 \$\pm\$ 0.1	81.4 \$\pm\$ 0.4	71.5 \$\pm\$ 0.2
	Model Soups/DiWA [†]	69.2	59.0	80.6	<u>82.2</u>	72.8
Our runs	Inter-training [31]	65.3 \$\pm\$ 0.3	55.8 \$\pm\$ 2.2	78.6 \$\pm\$ 0.1	80.1 \$\pm\$ 0.2	69.9 \$\pm\$ 0.6
	Ensemble* of inter-training	67.8 \$\pm\$ 0.1	60.5 \$\pm\$ 0.1	80.5 \$\pm\$ 0.2	82.0 \$\pm\$ 0.2	72.7 \$\pm\$ 0.1
	Fusing [35]	66.4 \$\pm\$ 0.5	59.8 \$\pm\$ 1.2	78.8 \$\pm\$ 0.2	81.0 \$\pm\$ 0.3	71.5 \$\pm\$ 0.5
	Recycling	69.8 \$\pm\$ 0.1	60.3 \$\pm\$ 0.2	80.4 \$\pm\$ 0.1	81.8 \$\pm\$ 0.2	73.1 \$\pm\$ 0.1
	Recycling	70.0 \$\pm\$ 0.2	60.8 \$\pm\$ 1.0	80.6 \$\pm\$ 0.1	82.0 \$\pm\$ 0.2	<u>73.4</u> \$\pm\$ 0.3
	Recycling [†]	70.4	60.7	80.6	<u>82.3</u>	73.5

Table 6: Accuracy (%,\$\uparrow\$) on TerraIncognita (best in **bold** and second underlined).

Algorithm	Selection	L100	L38	L43	L46	Avg
ERM	ID val	49.8 \$\pm\$ 4.4	42.1 \$\pm\$ 1.4	56.9 \$\pm\$ 1.8	35.7 \$\pm\$ 3.9	46.1 \$\pm\$ 1.8
CORAL [61]	ID val	51.6 \$\pm\$ 2.4	42.2 \$\pm\$ 1.0	57.0 \$\pm\$ 1.0	39.8 \$\pm\$ 2.9	47.6 \$\pm\$ 1.0
SWAD [52]	Loss-aware trajectory	55.4 \$\pm\$ 0.0	44.9 \$\pm\$ 1.1	59.7 \$\pm\$ 0.4	39.9 \$\pm\$ 0.2	50.0 \$\pm\$ 0.3
MA [27]	Uniform trajectory	54.9 \$\pm\$ 0.4	45.5 \$\pm\$ 0.6	60.1 \$\pm\$ 1.5	40.5 \$\pm\$ 0.4	50.3 \$\pm\$ 0.5
Deep ensembles* [27]	Uniform	53.0	42.6	60.5	40.8	49.2
DiWA[30] runs	ERM	59.9 \$\pm\$ 4.2	46.9 \$\pm\$ 0.9	54.6 \$\pm\$ 0.3	40.1 \$\pm\$ 2.2	50.4 \$\pm\$ 1.8
	Ensemble*	55.6 \$\pm\$ 1.4	45.4 \$\pm\$ 0.4	61.0 \$\pm\$ 0.4	41.3 \$\pm\$ 0.3	50.8 \$\pm\$ 0.5
	Model Soups/DiWA	56.3 \$\pm\$ 1.9	49.4 \$\pm\$ 0.7	59.9 \$\pm\$ 0.4	39.8 \$\pm\$ 0.5	51.4 \$\pm\$ 0.6
	Model Soups/DiWA	<u>58.5</u> \$\pm\$ 2.2	48.2 \$\pm\$ 0.3	58.5 \$\pm\$ 0.3	41.1 \$\pm\$ 1.2	51.6 \$\pm\$ 0.9
	Model Soups/DiWA [†]	57.2	<u>50.1</u>	60.3	39.8	51.9
Our runs	Inter-training [31]	49.9 \$\pm\$ 1.7	44.3 \$\pm\$ 1.6	54.7 \$\pm\$ 0.4	37.9 \$\pm\$ 1.1	46.7 \$\pm\$ 0.1
	Ensemble* of inter-training	58.1 \$\pm\$ 0.2	43.8 \$\pm\$ 0.4	61.0 \$\pm\$ 0.2	41.3 \$\pm\$ 0.4	51.1 \$\pm\$ 0.3
	Fusing [35]	52.8 \$\pm\$ 3.2	43.2 \$\pm\$ 2.3	55.2 \$\pm\$ 1.3	35.5 \$\pm\$ 0.3	46.7 \$\pm\$ 1.8
	Recycling	57.9 \$\pm\$ 0.2	<u>50.1</u> \$\pm\$ 0.7	59.8 \$\pm\$ 0.1	38.9 \$\pm\$ 0.5	51.8 \$\pm\$ 0.4
	Recycling	54.0 \$\pm\$ 2.0	47.7 \$\pm\$ 0.8	57.3 \$\pm\$ 0.8	37.9 \$\pm\$ 1.2	49.2 \$\pm\$ 0.9
	Recycling [†]	57.9	50.6	60.2	39.2	52.0

Table 7: Accuracy (%,\$\uparrow\$) on DomainNet (best in **bold** and second underlined).

Algorithm	Selection	Clipart	Info	Painting	QuickDraw	Photo	Sketch	Avg
ERM	ID val	58.1 \$\pm\$ 0.3	18.8 \$\pm\$ 0.3	46.7 \$\pm\$ 0.3	12.2 \$\pm\$ 0.4	59.6 \$\pm\$ 0.1	49.8 \$\pm\$ 0.4	40.9 \$\pm\$ 0.1
CORAL [61]	ID val	59.2 \$\pm\$ 0.1	19.7 \$\pm\$ 0.2	46.6 \$\pm\$ 0.3	13.4 \$\pm\$ 0.4	59.8 \$\pm\$ 0.2	50.1 \$\pm\$ 0.6	41.5 \$\pm\$ 0.1
SWAD [52]	Loss-aware trajectory	66.0 \$\pm\$ 0.1	22.4 \$\pm\$ 0.3	53.5 \$\pm\$ 0.1	16.1 \$\pm\$ 0.2	65.8 \$\pm\$ 0.4	55.5 \$\pm\$ 0.3	46.5 \$\pm\$ 0.1
MA [27]	Uniform trajectory	64.4 \$\pm\$ 0.3	22.4 \$\pm\$ 0.2	53.4 \$\pm\$ 0.3	15.4 \$\pm\$ 0.1	64.7 \$\pm\$ 0.2	55.5 \$\pm\$ 0.1	46.0 \$\pm\$ 0.1
Deep ensembles* [27]	Uniform	68.3	23.1	54.5	16.3	66.9	57.0	47.7
DiWA[30] runs	ERM	63.4 \$\pm\$ 0.2	21.1 \$\pm\$ 0.4	50.7 \$\pm\$ 0.3	13.5 \$\pm\$ 0.4	64.8 \$\pm\$ 0.4	52.4 \$\pm\$ 0.1	44.3 \$\pm\$ 0.2
	Ensemble*	66.7 \$\pm\$ 0.4	22.2 \$\pm\$ 0.1	54.1 \$\pm\$ 0.2	15.1 \$\pm\$ 0.2	68.4 \$\pm\$ 0.1	55.7 \$\pm\$ 0.2	47.0 \$\pm\$ 0.2
	Model Soups/DiWA	65.9 \$\pm\$ 0.4	23.0 \$\pm\$ 0.2	55.0 \$\pm\$ 0.3	16.1 \$\pm\$ 0.2	68.4 \$\pm\$ 0.1	55.7 \$\pm\$ 0.4	47.4 \$\pm\$ 0.2
	Model Soups/DiWA	66.7 \$\pm\$ 0.2	23.3 \$\pm\$ 0.2	55.3 \$\pm\$ 0.1	16.3 \$\pm\$ 0.2	68.2 \$\pm\$ 0.0	<u>56.2</u> \$\pm\$ 0.1	47.7 \$\pm\$ 0.1
	Model Soups/DiWA [†]	66.2	23.3	<u>55.4</u>	16.5	68.7	56.0	47.7
Our runs	Inter-training [31]	63.5 \$\pm\$ 0.1	21.1 \$\pm\$ 0.1	51.2 \$\pm\$ 0.2	14.2 \$\pm\$ 0.2	64.7 \$\pm\$ 0.3	52.1 \$\pm\$ 0.1	44.5 \$\pm\$ 0.1
	Ensemble* of inter-training	66.8 \$\pm\$ 0.2	22.3 \$\pm\$ 0.0	54.2 \$\pm\$ 0.2	15.4 \$\pm\$ 0.2	68.3 \$\pm\$ 0.0	55.8 \$\pm\$ 0.2	47.2 \$\pm\$ 0.1
	Fusing [35]	63.6 \$\pm\$ 0.1	21.3 \$\pm\$ 0.1	51.4 \$\pm\$ 0.2	14.0 \$\pm\$ 0.2	64.1 \$\pm\$ 0.4	52.1 \$\pm\$ 0.3	44.4 \$\pm\$ 0.2
	Recycling	65.9 \$\pm\$ 0.2	23.0 \$\pm\$ 0.1	55.1 \$\pm\$ 0.0	16.5 \$\pm\$ 0.1	68.3 \$\pm\$ 0.0	55.8 \$\pm\$ 0.0	47.5 \$\pm\$ 0.1
	Recycling	66.5 \$\pm\$ 0.1	23.2 \$\pm\$ 0.1	55.3 \$\pm\$ 0.0	16.7 \$\pm\$ 0.1	68.0 \$\pm\$ 0.0	56.0 \$\pm\$ 0.0	47.7 \$\pm\$ 0.0
	Recycling [†]	66.1	23.1	55.5	16.7	<u>68.5</u>	56.0	47.7